

Relation of susceptibility-weighted imaging findings with histological grade in intracranial meningiomas

 Mustafa Bozdog,  Ali Er

Department of Radiology, Tepecik Training and Research Hospital, Izmir, Turkey

Copyright@Author(s) - Available online at www.annalsmedres.org

Content of this journal is licensed under a Creative Commons Attribution-NonCommercial 4.0 International License.



Abstract

Aim: We aimed to investigate the relation of susceptibility-weighted imaging (SWI) findings with histological grade in intracranial meningiomas.

Materials and Methods: Histopathologically confirmed 58 intracranial meningioma patients (48 typical (low-grade meningioma), 10 atypical (high-grade meningioma)) who had undergone preoperative SWI between 2015 and 2020 were retrospectively evaluated. Tumor size, location, presence of peritumoral edema, WHO grade, low-grade meningioma subtypes and Ki-67 proliferation indexes were noted. SWI findings of intracranial meningiomas were categorized as either positive or negative based on presence/absence of intratumoral susceptibility signals (ITSSs). The origin of ITSSs in SWI-positive meningiomas was assessed with phase images and classified as calcification (SWI-C), vascular structure (SWI-V) or hemorrhage (SWI-H). Mann-Whitney U, chi-square, Fisher's exact tests and multiple logistic regression analyses were performed for statistical assessment.

Results: There was a significant association between SWI-positivity and low-grade in meningiomas ($p = 0.010$). A higher incidence of calcification was found in low-grade meningiomas (%60 in low-grade vs %10 in high-grade). Peritumoral edema was found to be associated with high grade in meningiomas ($p = 0.032$). Ki-67 proliferation index was significantly higher in high-grade meningiomas compared to low-grade. ($p = 0.000$).

Conclusion: SWI combined with peritumoral edema may help to predict high grade in intracranial meningiomas.

Keywords: Grade; magnetic resonance imaging; meningioma; susceptibility-weighted imaging

INTRODUCTION

Meningiomas are the most common type of primary brain tumors and constitute 24-30% of intracranial tumors (1). Meningiomas are classified as grade I (typical), grade II (atypical) and grade III (anaplastic) in the classification of the central nervous system (CNS) tumors of the world health organization (WHO) (2). WHO grade I meningiomas constitute low grade meningiomas (LGM); on the other hand WHO grade II and III meningiomas constitute high grade meningiomas (HGM). The curative treatment of meningiomas is surgical and as the histological grade increases, tumor recurrence rate increases and this situation reduces the long-term survival rates (3). Tumor recurrence is an indicator of poor prognosis and is associated with histological grade (4). Therefore, there are important clinical implications of distinguishing between high and low grades in pre-treatment of meningiomas.

In contrast magnetic resonance imaging (MRI), the diagnosis of intracranial meningiomas is straightforward due to its typical features such as extra-axial location,

dural tail mark and homogeneous enhancement (5). Although conventional MRI gives valuable information about the location, size and invasion of adjacent tissues, the information it provides on histological grade with prognostic significance remains limited. Susceptibility-weighted imaging (SWI), one of the advanced MRI applications, can provide more information about the internal structure of the lesions (6). SWI is basically a high-resolution, flow-compensated, 3D gradient echo-imaging technique that uses both magnitude and filtered phase information in each voxel to enhance contrast in MRI (6-8). Thus, it offers valuable information about any tissue that has a different susceptibility from its surrounding structures such as calcium, deoxygenated blood and hemosiderin (8). These structures appear black in the form of susceptibility signals in the SWI sequence (9). In this way, intratumoral microvascular structures, hemorrhage products and calcifications can be shown in neoplasms with SWI (7-9). Thus, intratumoral SWI findings can provide information about the structure and histological grade of the tumor. In previous publications, SWI has proven to be a

Received: 11.06.2020 Accepted: 12.08.2020 Available online: 22.04.2021

Corresponding Author: Mustafa Bozdog, Department of Radiology, Tepecik Training and Research Hospital, Izmir, Turkey

E-mail: bozdogmustafa.84@gmail.com

valuable imaging method in assessing and differentiating the grade of intracranial tumors (10-14).

In our study we aimed to investigate the relation of SWI findings with histological grade in intracranial meningiomas.

MATERIALS and METHODS

Patients

Patients who were operated in our hospital between January 2015 and April 2020 and histopathologically diagnosed with intracranial meningioma were scanned in the hospital database. Scanning result found 134 cases. Radiology images of these cases were examined. In addition to contrast-enhanced MRI examination, SWI imaging was performed in 66 cases. The SWI sequences of these cases were analyzed retrospectively. Three cases were excluded from the evaluation because the meningioma was smaller than 1 cm. In addition, 5 cases were excluded from the study due to the intense susceptibility artifacts caused by paranasal sinus air adjacent to the meningioma masses located in the suprasellar and olfactory groove. As a result, 58 patients (37 females, 21 males), with a histopathological diagnosis of meningioma who underwent SWI preoperatively were included. Histopathological diagnoses and Ki-67 proliferation index (PI) levels were obtained from the hospital database. This retrospective was approved by University of Health Sciences Tepecik Training and Research Hospital Local Ethics Committee (approval date: 23.07.2020, protocol no: 2020/9-8).

MRI protocol

All brain MRI examinations of the patients were performed on a 1.5 Tesla (T) MRI scanner using the head coil (Aera, Siemens, Erlangen, Germany). During the same procedure, patients were imaged with conventional MRI and SWI sequences. SWI was performed before the contrast medium was administered. Conventional MRI protocol was as fluid-attenuated inversion recovery (FLAIR), multiplanar T1-weighted (W) and T2-weighted (W) spin-echo (SE) sequences (Slice thickness = 5 mm, matrix size = 240 x 320, field of view; FOV= 23 cm). Contrast-enhanced examination was performed with T1W SE sequences in three plans following intravenous administration of paramagnetic contrast agent (gadopentetatedimeglumine, Magnevist; Bayer Schering Pharma, Leverkusen, Germany) at a bolus dose of 0.1 mg / kg. The parameters of the SWI sequence were TR / TE = 49 ms / 40 ms FOV = 21 cm, matrix size = 232 x 256, slice thickness = 2 mm, flip angle = 15°. Later, SWI sequences were restructured. Magnitude images, filtered-phase images, minimum intensity projection (MinIP) images and the latest SWI images were created. Also, all patients had preoperative noncontrast cranial computed tomography (CT) imaging.

Image Analysis

An experienced radiologist (A.E.) blinded to histopathological information of the cases evaluated conventional MRI and SWI sequences. In contrast-

enhanced T1A imaging, the longest diameter of the tumor was measured. The location of the tumor in the conventional MRI sequences (Supratentorial [skull base, convexity, falx] and infratentorial), the presence of peritumoral edema (absent or present) in the T2W and FLAIR sequences were noted. The presence of intratumoral susceptibility signals (ITSSs) in the SWI sequence was evaluated as SWI-positive or SWI-negative. In the presence of ITSS, the origin of susceptibility signals were interpreted by assessing the phase images and noncontrast cranial CT images. Cases with calcification were named as ITSS-C, cases with vascular structure were named as ITSS-V and cases with hemorrhage were named ITSS-H.

Statistical analysis

Statistical analysis was performed by SPSS 23.00 software program (IBM Corp., Armonk, N.Y., USA). Numerical data were expressed as mean \pm standard deviation and categorical data as frequency (%). The normal distribution of numerical data was evaluated by the Shapiro-Wilk test. Since the data were not normally distributed, the differences between continuous numerical data and histopathological findings were evaluated with the Mann-Whitney U test. The analysis of demographic (age and gender), radiological and histopathological categorical data across histological grades and subtypes of meningiomas were done with chi-square and Fisher's exact tests. A value of $p < 0.05$ was considered statistically significant.

RESULTS

Among the 58 meningiomas included in our study, histopathological analysis revealed 48 (83%) typical meningiomas (LGM) and 10 (17%) atypical meningiomas (HGM). Of the LGMs, 23 were of meningothelial subtype (48%), 8 transitional (17%), 8 fibrous (17%), 6 psammomatous (12%) and 3 angiomatous (6%) subtypes. Mean age was calculated as 60 ± 13 in male gender and 54 ± 12 in female gender and no significant difference was observed ($p = 0.217$). There was no significant difference between LGM and HGM groups in terms of age and tumor size ($p = 0.829$, $p = 0.113$, respectively). Peritumoral edema was observed in 15 (31%) of LGMs and 7 (70%) of HGMs. A weak but statistically significant relationship was found between the presence of peritumoral edema and high grade in meningioma ($p = 0.032$). No significant relationship was found between tumor size and peritumoral edema ($p = 0.168$). Of the meningiomas, 46 (79%) were supratentorial (30 were at convexity, 10 were at skull base, 6 were at the falx) and 12 (21%) were at the infratentorial location. There was no association between tumor localization and peritumoral edema ($p = 0.075$). In our study, ITSS was observed in 39 (67%) of 58 meningiomas and were evaluated as SWI-positive. SWI-positivity was detected in 36 (75%) of LGMs and 3 (30%) of HGMs. A statistically significant relationship was detected between SWI-positive findings and histopathological low grade of meningioma ($p = 0.010$).

Combining SWI-positivity and the absence of peritumoral edema, the analysis revealed a stronger relationship with histological low grade in meningiomas ($p = 0.004$). When SWI was evaluated with phase images; it was observed that ITSS belonged to calcification (ITSS-C) in 30 cases, vascular structures in 5 cases (ITSS-V) and hemorrhage in 4 cases (ITSS-H). Ki-67 PI levels were significantly higher in HGM compared to LGM ($p = 0.000$). Comparative data of LGM and HGM groups are shown in Table 1.

In LGMs, no statistically significant relationship between LGM subtypes peritumoral edema was demonstrated ($p = 0.093$). In addition, when LGM subtypes were evaluated individually, SWI-positivity was a common finding and did not help distinguish among LGM subtypes ($p = 0.065$). Also, Ki-67 PI levels were similar among LGM subtypes as well ($p = 0.655$).

Table 1. Comparison of patient age, gender, tumor size, peritumoral edema, SWI-positivity, ITSS types and Ki-67 index parameters between low-grade and high-grade meningiomas

Parameter	Low-grade meningioma (48)	High-grade meningioma (10)	p value
Age (years)	56 ± 12	58 ± 13	0.829
Gender (F/M)	32:16	5:5	0.318
Tumor size (cm)	3.5 ± 1.2	4.5 ± 1.2	0.113
Peritumoral edema	15 (%31)	7 (%70)	0.032
SWI-positivity	36 (%75)	3 (%30)	0.010
ITSS-C	29 (%60)	1 (%10)	
ITSS-V	5 (%10)	0	
ITSS-H	2 (%4)	2 (%20)	
Ki-67 (%)	2.9 ± 2.5	11 ± 6.8	0.000

Table 2. Comparison of parameters between low-grade meningioma subtypes

Subtype	Meningeothelial	Transitional	Fibrous	Psammomatous	Angiomatous	p-value
Number of cases	23 (%48)	8 (%17)	8 (%17)	6 (%12)	3 (%6)	
Peritumoral edema	7	2	2	1	3	0.093
SWI-positivity	15	6	6	6	3	0.065
ITSS-C	11	6	5	6	1	
ITSS-V	3	0	1	0	1	
ITSS-H	1	0	0	0	1	
Ki-67 (%)	3.2±2.8	2.8±1.8	3.6±2.8	1.2±0.4	2±1.7	0.655

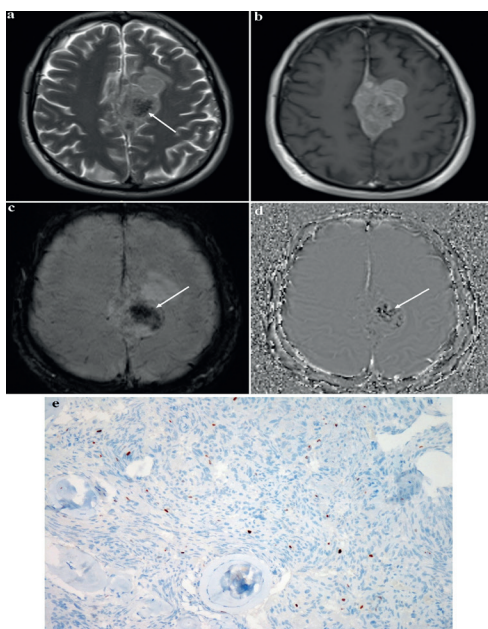


Figure 1. MRI of a 65-year-old man with low-grade meningioma located at the para-falcine region. Axial T2W image (a) reveals hypointensity (white arrow) within the tumor and axial contrast-enhanced T1W image (b) demonstrates an intense enhancement. Susceptibility-weighted image (c) shows intratumoral susceptibility signals (ITSSs) as hypointense areas (white arrow). ITSSs display hypointense (white arrow) on corresponding phase image (d) that confirm the presence of coarse calcifications within tumor. The photomicrograph (e) shows the histology low-grade meningioma (transitional) and 5% immunohistochemical staining level for the Ki-67 proliferation index

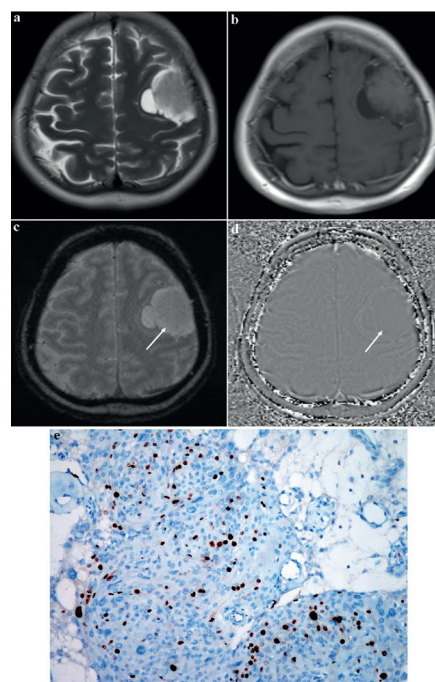


Figure 2. MRI of a 49-year-old woman with high-grade meningioma (atypical) located at right frontal convexity. The tumor is isointense on axial T2W image (a) and shows a mild homogeneous enhancement on axial contrast-enhanced T1W image (b). ITSS was absent within the tumor (white arrows) on susceptibility-weighted image (c) and corresponding phase image (d). The photomicrograph (e) shows the histology of atypical meningioma (WHO grade II) and 20% immunohistochemical staining level for the Ki-67 proliferation index

Detailed data and ITSS distribution in LGM subtypes are shown in Table 2. No significant correlation was observed between Ki-67 PI and tumor size ($p = 0.636$). There was no significant difference in Ki-67 PI levels between patients with SWI-positive meningioma and those without ($p = 0.132$). LGM and HGM representation cases are shown in Figures 1 and 2, respectively.

DISCUSSION

Accurate evaluation of histological grade with preoperative imaging methods in intracranial meningiomas is important as it affects the treatment approaches and prognosis of patients. In our study, we investigated the relationship between the findings in the SWI sequence of intracranial meningiomas and histological grade and LGM subtypes. The cases with ITSSs in the SWI sequence were evaluated as SWI-positive. SWI-positive findings were observed in 36 of 48 LGM cases. We found that the SWI-positive finding was associated with low grade in meningiomas ($p = 0.010$). Considering the correlation with phase images, we found that the incidence of calcification was higher in low-grade meningiomas (60% in LGMs vs. 10% in HGMs). Tumor calcification is a common feature of LGMs and a negative correlation has been shown between calcification and growth rate in previous publications (15). In another study, it was stated that the absence of calcification was one of the imaging features most associated with high grade in meningiomas (16). CT has an important role in detecting calcification. However, the most important disadvantage of CT compared to MRI is the increase in cancer risk due to radiation exposure. Adams et al. showed that SWI is a highly reliable imaging method in detecting intracranial meningioma-related calcifications and has higher diagnostic accuracy than standard MRI sequences (17).

Three of the cases with ITSSs detected in LGM were angiomatous subtype. Angiomatous subtype is known for its hypervascular feature. Among angiomatous subtype, ITSSs were observed in favor of vascular structures in one case, hemorrhage in one case and calcification in one case. In other LGM subtypes, ITSS-C was a common finding, while in meningothelial subtype, besides ITSS-C, ITSSs were detected in favor of microhemorrhage and vascularity in four meningioma cases. In our study, although gross hemorrhage was not observed in meningiomas, it was observed that intratumoral microhemorrhages were not very rare. There is a need for further verification of our data by further studies with SWI in meningiomas. While SWI was negative in 7 cases in HGM; in 2 of 3 other SWI positive cases, ITSS-H was observed in linear morphology at the periphery of the cystic-necrotic area (Figure 3). Compared to LMGs, HGMs are expected to be more likely to bleed. However, in our study, no significant relationship was found between hemorrhage and meningioma grade. In a recent study published in the literature, they stated that hemorrhage detected in SWI did not contribute to differentiating high and low grade in meningioma, in accordance with our study (18). Depending on the

subtype of the meningioma, the vascular, hemorrhagic and calcific components of the tumor can vary and show heterogeneity, regardless of grade. The distribution of meningioma grades and subtypes in studies may lead to different statistical results. For example, the inclusion of the psammomatous meningioma, known for its calcification feature, as in our study, may have caused bias in our findings.

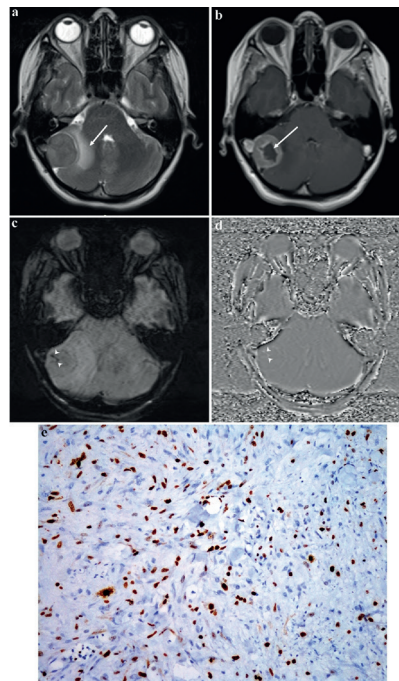


Figure 3. MRI of a 50-year-old woman with high-grade meningioma (atypical) located at right cerebellar convexity. Axial T2W image (a) reveals peritumoral edema as hyperintense areas (white arrow). Axial contrast-enhanced T1W image (b) demonstrates a lack of enhancement (white arrow) representing cystic/necrotic area within the tumor. Susceptibility-weighted image (c) shows fine linear susceptibility signals (white arrow) at the periphery of non-enhanced region of the tumor. Corresponding phase image (d) shows susceptibility signals as hyperintense structures (white arrow heads) representing microhemorrhage within the tumor. The photomicrograph (e) shows histology of atypical meningioma (WHO grade II) and 25% immunohistochemical staining level for the Ki-67 proliferation index

In our study, we found a statistically significant relationship between the presence of peritumoral edema and HGM ($p = 0.032$). This finding was compatible with previous studies in the literature (18-20). It is observed that the edema is vasogenic in diffusion-weighted imaging. The tumor-secreted vascular endothelial growth factor (VEGF)-induced pial vascularity and tumor vascularity are thought to cause brain edema (21,22). Peritumoral edema is not uncommon in meningiomas and in our study, approximately 1/3 of LGMs demonstrated peritumoral edema. The relationship between peritumoral edema and meningioma grade was not strong. The distribution and number of meningioma grades and LGM subtypes in different studies may cause conflicting results in terms of relationship between peritumoral edema and meningioma grade. Thus, some previous studies could not elaborate

a significant relationship (23-25). Current study achieved a stronger level of significance in terms of meningioma grades by combining the parameter peritumoral edema with SWI findings ($p = 0.004$). Zhang et al. reported that although peritumoral edema was useful in predicting HGM, adding the SWI findings did not contribute to this distinction and found a different result from our study (18). We think that this difference may be due to the aforementioned reasons. In addition, Zang et al. employed quantitative susceptibility mapping for assessment in their study (18). Mapping method was not utilized in our study. This variation in method may have resulted in different results.

Although Ki-67 PI, which reflects cellular proliferation and is widely used in clinical use, is not one of the histological grading criteria in the WHO classification, high Ki-67 PI levels generally indicate a high grade in meningioma (26). Indeed, in our study, Ki-67 levels were found to be significantly higher in HGMs than in low-grade. There was no significant difference in Ki-67 PI levels between SWI-positive and SWI-negative groups regardless of histological grade. We expected no relation between SWI and Ki-67, which provides limited information about tumor cellularity.

Apart from being retrospective, our study had other limitations. First of all, a small number of patients were enrolled in the study with a great selection bias. The number of atypical meningiomas evaluated as HGM was very low, and we had no anaplastic meningioma (grade 3) cases. The reason for this was the fact that all of our cases had histopathological diagnosis which is the most important strength of our study. In this way, we had the opportunity to analyze with histopathological findings. In a SWI study with a large number of meningioma cases in the literature, the diagnosis of meningioma was made with imaging findings and histopathological diagnoses were not available (16). Secondly, we evaluated ITSS as SWI-positive / negative, not by scoring semiquantitatively. We found that only hemorrhagic type ITSS was evaluated in semiquantitative analysis (12,14). Since it may be important in histopathological distinction; we also included the frequent calcification feature of meningioma into the analysis. Since calcification in meningiomas can be presented in diffuse or amorphous morphology; ITSS evaluation could not be done by semi-quantitative scoring method. Thirdly, since cases were evaluated by a single radiologist, inter-observer variability was not taken into account.

CONCLUSION

In conclusion, peritumoral edema with the inclusion of SWI results demonstrated a stronger relationship with histological grade in intracranial meningiomas. The presence of ITSS due to calcification in SWI; supports low grade in meningioma. Studies involving more cases and meningioma grades / subtypes are needed.

Competing interests: The authors declare that they have no competing interest.

Financial Disclosure: There are no financial supports.

Ethical approval: This study was approved by the Clinical Research Committee of University of Health Sciences Tepecik Training and Research Hospital and conducted in compliance with the ethical principles according to the Declaration of Helsinki (Protocol No: 2020/9-8).

REFERENCES

1. Chamoun R, Krisht KM, Couldwell WT. Incidental meningiomas. *Neurosurg Focus* 2011;31:19.
2. Louis DN, Perry A, Reifenberger G, et al. The 2016 World Health Organization classification of tumors of the central nervous system: a summary. *Acta Neuropathol* 2016;131:803-20.
3. Claus EB, Bondy ML, Schildkraut JM, et al. Epidemiology of intracranial meningioma. *Neurosurgery* 2005;57:1088-95.
4. Riemenschneider MJ, Perry A, Reifenberger G. Histological classification and molecular genetics of meningiomas. *Lancet Neurol* 2006;5:1045-54.
5. Watts J, Box G, Galvin A, et al. Magnetic resonance imaging of meningiomas: a pictorial review. *Insights Imaging* 2014;5:113-22.
6. Mittal S, Wu Z, Neelavalli J, et al. Susceptibility-weighted imaging: technical aspects and clinical applications, part 2. *AJNR Am J Neuroradiol* 2009;30:232-52.
7. Haacke EM, Xu Y, Cheng YC, et al. Susceptibility-weighted imaging (SWI). *Magn Reson Med* 2004;52:612-8.
8. Haacke EM, Mittal S, Wu Z, et al. Susceptibility weighted imaging: technical aspects and clinical applications, part 1. *AJNR Am J Neuroradiol* 2009;30:19-30.
9. Chen W, Zhu W, Kovanlikaya I, et al. Intracranial calcifications and hemorrhages: characterization with quantitative susceptibility mapping. *Radiology* 2014;270:496-505.
10. Ding Y, Xing Z, Liu B, et al. Differentiation of primary central nervous system lymphoma from high-grade glioma and brain metastases using susceptibility-weighted imaging. *Brain Behav* 2014;4:841-9.
11. Kim HS, Jahng GH, Ryu CW, et al. Added value and diagnostic performance of intratumoral susceptibility signals in the differential diagnosis of solitary enhancing brain lesions: preliminary study. *Am J Neuroradiol* 2009;30:1574-9.
12. Yu Y, Zhang H, Xiao Z, et al. Diffusion-weighted MRI combined with susceptibility-weighted MRI: added diagnostic value for four common lateral ventricular tumors. *Acta Radiol* 2018;59:980-7.
13. Saini J, Gupta PK, Sahoo P, et al. Differentiation of grade II/III and grade IV glioma by combining "T1 contrast enhanced brain perfusion imaging" and susceptibility-weighted quantitative imaging. *Neuroradiology* 2018;60:43-50.

14. Chen T, Jiang B, Zheng Y, et al. Differentiating intracranial solitary fibrous tumor/hemangiopericytoma from meningioma using diffusion-weighted imaging and susceptibility-weighted imaging. *Neuroradiology* 2020;62:175-84.
15. Oya S, Kim SH, Sade B, et al. The natural history of intracranial meningiomas. *J Neurosurg* 2011;114:1250-6.
16. Hwang WL, Marciscano AE, Niemierko A, et al. Imaging and extent of surgical resection predict risk of meningioma recurrence better than WHO histopathological grade. *Neuro Oncol* 2016;18:863-72.
17. Adams LC, Böker SM, Bender YY, et al. Assessment of intracranial meningioma-associated calcifications using susceptibility-weighted MRI. *J Magn Reson Imaging* 2017;46:1177-86.
18. Zhang S, Chiang GC, Knapp JM, et al. Grading meningiomas utilizing multiparametric MRI with inclusion of susceptibility weighted imaging and quantitative susceptibility mapping. *J Neuroradiol* 2020;47:272-7.
19. Liang RF, Xiu YJ, Wang X, et al. The potential risk factors for atypical and anaplastic meningiomas: clinical series of 1,239 cases. *Int J Clin Exp Med* 2014;7:5696-700.
20. Hale AT, Wang L, Strother MK, et al. Differentiating meningioma grade by imaging features on magnetic resonance imaging. *J Clin Neurosci* 2018;48:71-5.
21. Pistolesi S, Fontanini G, Camacci T, et al. Meningioma associated brain oedema: the role of angiogenic factors and pial blood supply. *J Neurooncol* 2002;60:159-64.
22. Osawa T, Tosaka M, Nagaishi M, et al. Factors affecting peritumoral brain edema in meningioma: special histological subtypes with prominently extensive edema. *J Neurooncol* 2013;111:49-57.
23. Hsu C-C, Pai C-Y, Kao H-W, et al. Do aggressive imaging features correlate with advanced histopathological grade in meningiomas? *J Clin Neurosci* 2010;17:584-7.
24. Li H, Zhao M, Jiao Y, et al. Prediction of high-grade pediatric meningiomas: magnetic resonance imaging features based on T1-weighted, T2-weighted, and contrast-enhanced T1-weighted images. *World Neurosurg* 2016;91:89-95.
25. Watanabe Y, Yamasaki F, Kajiwara Y, et al. Preoperative histological grading of meningiomas using apparent diffusion coefficient at 3T MRI. *Eur J Radiol* 2013;82:658-63.
26. Mukhopadhyay M, Das C, Kumari M, et al. Spectrum of meningioma with special reference to prognostic utility of ER, PR and Ki67 expression. *J Lab Physicians* 2017;9:308-13.